

Titania Thin Films and Supported Nanostructured Membranes Prepared by the Surfactant Assisted Sol-Gel Method

P. Kluson^{*a}, P. Kacer^a, T. Cajthaml^b and M. Kalaji^c

^aFaculty of Chemical Technology, Institute of Chemical Technology Prague, Technicka 5, 166 28 Prague, Czech Republic

^bInstitute of Microbiology, Academy of Sciences of Czech Republic, Videnska 1083, 142 20 Prague, Czech Republic

^cDepartment of Chemistry, University of Wales in Bangor, Gwynedd LL57 2UW, United Kingdom

Original scientific paper

Received: October 28, 2002

Accepted: March 1, 2003

Thin TiO₂ nanoparticulate layers were produced by a dip coating of quartz, boron-silicate wafers and of plastic foils. The coating solution was prepared by the sol-gel method in the reverse micelle environment to favour the polycondensation. Reverse micelles of a non-ionic surfactant Triton X-100 in cyclohexane were used as the template. The molar ratio water/surfactant was kept low ($r = 1$). At this ratio water molecules were associated only with terminal groups of the hydrophilic chains in the micelle aggregate. Polymeric precursor layers were thermally treated to obtain the desired thin films of anatase. Direct thermal decomposition of the organic content was replaced by supercritical fluid extraction followed by the thermal treatment. The data showed that supercritical fluid extraction considerably reduced the organic carbon content and provided a surface structure closely similar to that of anatase. A similar procedure was used to obtain a titania membrane supported on a plankton based silica matrix.

Keywords:

Titanium oxide, nanostructures, surfactant templating, thin films, micro-membrane, photocatalysis, solar-cells

Introduction

Photooxidation of organic pollutants either in the gas or the liquid phase on various TiO₂ (titania) catalysts has attracted the attention of many research groups over the past ten years.^{1–27} Among the various types of titania those used as thin films are very promising.^{1–5,10,25,28–36} Their practical utilisation does not obviously involve an expensive separation, compared to oxidation processes that are carried out in slurries. The thin films, which are usually particulate in nature, retain the photophysical and photochemical properties of individual semiconductor particles. This is due to the fact that their mode of action is identical to that of particles in suspension.^{2,25,34,35} The performance of titania films as photocatalysts invariably depends on the surface and the structural properties which are functions of the preparation method. Sol-gel transformation has been used in the past^{e.g.,37} for the preparation of high surface area oxides (mostly silica). However, alkoxides of transition metals hydrolyse rapidly yielding precipitates containing non-uniform large particles. If the hydrolysis is restrained in favour of polycondensation a polymeric network

(a precursor of the structure of homogeneous nanoparticles) could develop. Surfactant assisted sol-gel (reverse micelles) preparation of titania nanoparticles has been recently reported.^{34,35,38} In this process the alkoxide hydrolyses in a core of a reverse micelle with a limited amount of water. Then the polycondensation step could proceed simultaneously^{34,35,39,40} and is highly competitive.^{17,35,41–43} It provides particles with a unique monodisperse structure uniform in dimension and shape.

In this work we report on the generation of titania precursor gels within templates of assemblies of reverse micelles of the non-ionic surfactant Triton X-100 in cyclohexane. The precursors are used at an early stage of the gelling process during the dip coating of glass and quartz wafers and of polyvinylacetate (PVA) foils. The physical and chemical properties of the ensembles are discussed in terms of their prospective utilisation as new generation photoactive catalysts for the oxidation of organic molecules. Attention has been paid to methods of the gel transformation and to the conditions of formation of the final titania particles. The direct thermal treatment was replaced by supercritical fluid extraction^{44,45} followed by the thermal decomposition of the residual organic carbon content. The same procedure is also applied for the coating of the plankton based silica matrix with nanostructured titania.

* corresponding author (e-mail P.Kluson@seznam.cz, phone 00420 224 35 3769; fax 00420 224 31 1968)

Experimental part

Preparation of a gel

Reverse micelles of a non-ionic surfactant ($C_{33}H_{60}O_{10.5}$) with a long hydrophilic poly(oxyethylene) chain^{46–47} Triton X-100 (Aldrich, 99.99 %) in cyclohexane (Aldrich, HPLC grade, water content less than 0.01 %), were used.^{34,35,46–50} The molar ratio of water (millipore water) to surfactant $r = 1$ was kept constant throughout all experiments. Up to this value water molecules are predominantly associated with the terminal hydroxyl groups.^{35,50} The approximate composition of TX-100 was 0.85 mol kg⁻¹ and the alkoxide used was titanium(IV)-isopropoxide (TIOP) (Aldrich, 99.99 %). For the sake of comparison thin layers were also prepared by the sol-gel method using a coating solution without the surfactant and with a composition 2-propanol (Fluka, HPLC grade, water content less than 0.02 %), TIOP and water (dried at 353K).

Dip coating

Quartz and boron-silicate glass wafers and PVA foils were employed as substrates for the dip coating.^{2–5,8,10,16,25,26,31,34–36,51,52} The wafers were washed in sulphuric acid (0.5 mol dm⁻³), then soaked in an alkaline solution (NaOH, pH 12) and finally treated in an ultrasonic bath for 15 min in water (PVA foils only sonicated). Wafers as well as the foils were removed from the gelling solution at a constant speed of 6 cm min⁻¹. The samples were allowed to stay in a vertical position for 3 min in a box with a controlled humidity (35 %) and then dried in air (303 K) for the next 3 min. Thicker layers were prepared by repeating this process.

Temperature programmed reduction (TPR) and thermogravimetric analysis (TGA)

Fresh gel layers were allowed to stay open to air at 323 K for 2 h (ageing, after this noted as raw gels). Then, with the exception of films deposited on a PVA foil, the organic content⁵³ was thermally decomposed in a furnace in air ($Q = 40$ cm³ min⁻¹) at 8 isothermal levels (interval 423 K to 873 K). Gaseous products were analysed by mass spectroscopy (Saturn 2000, Varian). Solid fractions remaining on wafers at each temperature level were extracted by toluene and methanol and analysed. The effect of temperature on supported gels was also studied using a TGA apparatus TG 750 (Stanton & Redcroft) at a rate of heating of 20 °C min⁻¹ in air (10 ml min⁻¹) with samples positioned in a platinum holder.

Supercritical fluid extraction

Supercritical fluid extraction (SFE) was performed in a Suprex extractor using carbon dioxide (SFE grade, Messer Griesheim) at 45.6 MPa and at 373 K for 180 min. The thin layers were then analysed for their carbon content using elemental analysis (Perkin-Elmer, CHN-240C).

X-ray diffraction (XRD) analysis

Crystallographic phase structure^{54–57} of the TiO₂ layers was determined in the low-angle incident mode by XRD (R. Seifert Co.) using Bragg-Brentan focusing geometry, CoK α radiation and a graphite monochromator.

SEM and ellipsometry

Images of thin films were recorded using a Hitachi S-520 SEM apparatus at $U = 14$ kV. Samples were fixed on a microscopy holder by a conductive carbon tape and sputtered with gold. Images were mostly used for evaluation of the film thickness. The thickness was also estimated by the ex-situ ellipsometry (also refractive indices) using a conventional rotating analyser (Sentech) fitted with a He-laser beam. The measurements were carried out at an angle of incidence of 70°. The layer thickness was evaluated from the change in ellipsometric parameters between the bare and the modified substrates for a three phase model (substrate-layer-air).

Infrared spectroscopy

Raw gels and precipitates prepared in the surfactant-free environment were analysed by IR spectroscopy. The spectra were recorded using a Nicolet 740 spectrometer.

XPS analysis

XPS analysis of gels after supercritical fluid extraction was carried out using an ESCA 310 spectrometer (Gammadata Scientia AB) with a rotational anode, monochromator, hemispheric analyser of electrons in a high vacuum (10⁻⁹ mbar), and an AlK α source of radiation ($h\nu = 1486.6$ eV) for electrons excitation.

UV-vis absorption spectroscopy

Ultraviolet-visible spectroscopy measurements (absorption mode) were carried out using a Perkin-Elmer Lambda 19 spectrometer with aim to assess a presence of small particle diameter effects.

Results and discussion

Recent data⁵⁷ describing the process of polymerisation revealed, that for the gel composition

used in this work, the gelling process was completed in approximately 120 min. As the intention of the work described here was to carry out the coating during the early stages of gelling, a period of 15 min after the addition of the alkoxide was chosen as a suitable period after which the dipping commenced. The same interval and composition were kept in any other coating cycle following the first one. The raw layers were well transparent and this property was preserved even with films prepared by ten coating cycles. Translucent white layers (due to the presence of the titanium hydroxide precipitate) would indicate prevailing hydrolysis and little extent of polycondensation. For comparison, SEM of such a layer prepared by a standard sol-gel routine (dried at 353 K) without the surfactant (2-propanol/TIOP/ water), is shown in Figure 1.

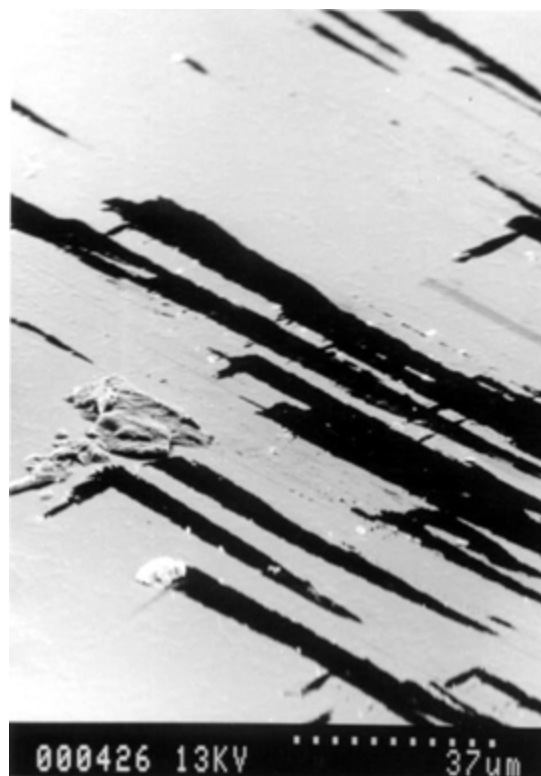


Fig. 1 – SEM image of a translucent thin layer prepared by sol-gel in the surfactant free environment (dried at 353 K). The image shows many “paths” (bare glass surface) originating from mechanically replaced precipitated particles.

Infrared spectra of a raw gel and a precipitate formed in the surfactant-free environment, are shown in Figure 2. The spectrum of the raw gel (fresh gel dried at 353 K) is characterised by absorbances typical for alkyl chains (2920 and 2850 cm^{-1}) and the ether linkage vibration centred at 1150 cm^{-1} (fingerprints of the surfactant). The increased intensity of the OH group at high numbers

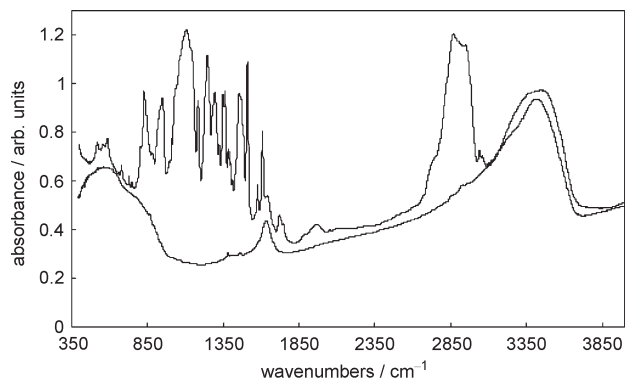


Fig. 2 – IR spectra of a raw gel layer (the upper spectrum) and of a thin layer formed from $\text{Ti}(\text{OH})_4$ precipitate prepared in the surfactant free environment (the lower spectrum)

is from occluded water and Ti-OH groups (also the bending mode of water (H_2O) at 1648 cm^{-1}). The spectrum of the precipitate reveals the characteristic structure of titania demonstrated by strong and broad absorbances between 500 and 900 cm^{-1} .

A TGA curve of a raw gel (10 layers deposited on quartz) is given in Figure 3. Evaporation of water and volatile organic molecules (cyclohexane) starts below 373 K and effectively terminates at 483 K. At 523 K a steep decline associated with an attack by oxygen on the poly(oxyethylene) chain and the terminal alkyl part of the hydrophobic head. Mass spectroscopy revealed carbon dioxide, acetaldehyde and acetone, as prominent products of this stage. The core of the hydrophobic part of the surfactant’s molecule is more resistant to oxidation. Up to 673 K it is stabilised through a quinone structure with a mass of 134 (formula $(\text{CH}_3)_2\text{C}=\text{C}_6\text{H}_4=\text{O}$). Above 673 K it is oxidised as indicated by the small “bump” on the TGA curve. The decomposition virtually terminates at 823 K, when the layer could be referred to as carbon-free.

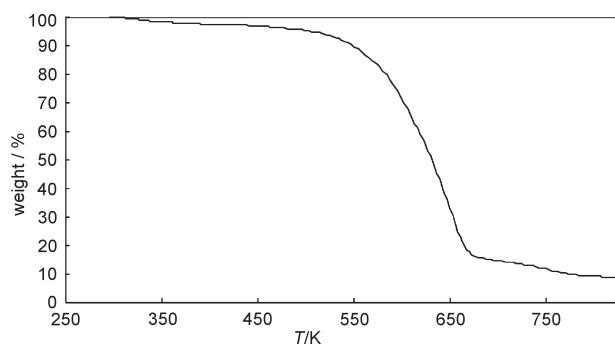


Fig. 3 – A TGA curve of the decomposition of the layer of a raw gel (10 layers deposited on quartz, weight of a bare support is excluded)

The XRD pattern of a layer treated at 573 K is completely flat; at 623 K an increased background

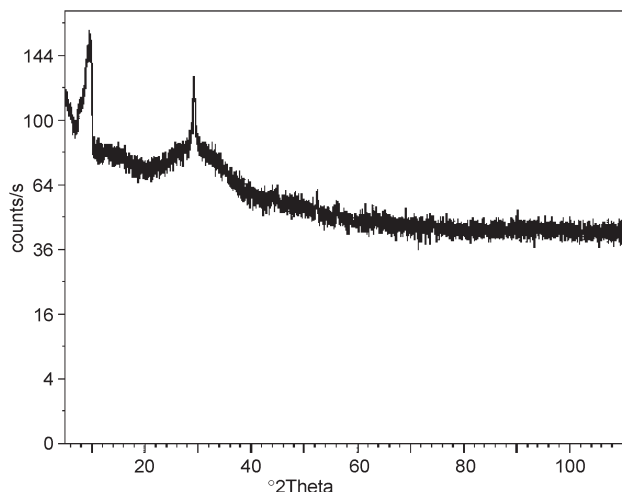


Fig. 4 – X-ray diffraction pattern of the anatase thin layer treated at 773 K in air. The bends located below $2\theta = 20^\circ$ are not due to TiO_2 and come from the XRD instrumentation.

around the most significant diffraction of anatase from the (101) plane, appears. At 723 K a short but already sharp peak centred at $2\theta = 29.4^\circ$ dominates the originally diffuse band and at 773 K this peak becomes even more prominent (Figure 4).

The layers treated at 823 K and above were less transparent due to the larger extent of crystallisation (e.g., micro-crystals of anatase in Figure 5-A obtained at 873 K could be compared



Fig. 5 A – SEM image of a translucent layer with well developed micro-crystals of anatase (873 K)

with the perfectly transparent film treated at 673 K in Figure 5-B).

The dependency of the film thickness on the number of coating cycles was linear (all samples treated at 673 K). The maximum thickness obtained by ten cycles was estimated from a set of micrographs to be approximately 405 nm, a thickness of a layer prepared in 8 steps was evaluated to be in average 328 nm. The five-cycle process provided layers from 199 to 210 nm. Images of layers from three coating cycles (e.g., Figure 5-B) revealed a thickness from 108 to 128 nm depending on the position of its evaluation. SEM images of a single layer were not taken due to the resolution limit of the microscopy instrumentation.

Besides microscopy this value was also estimated by ellipsometry. A thickness of 125 ± 2 nm was found for the film prepared using three cycles and 217 ± 1 nm for the five-cycle process. These results are in an excellent agreement with the microscopy-based estimation. The refractive index calculated at $\lambda = 630$ nm for the three-cycle layer was $n_f = 1.50 \pm 0.03$ of. The refractive index of crystalline anatase at the same wavelength was calculated at $n_c = 2.5$ (Ohya et.al.³¹). Therefore, the porosity of the thin layer calculated from the Lorentz-Lorentz equation^{e.g., 58} was 51 %.

Supercritical fluid extraction was chosen as an alternative method to the direct thermal treatment of

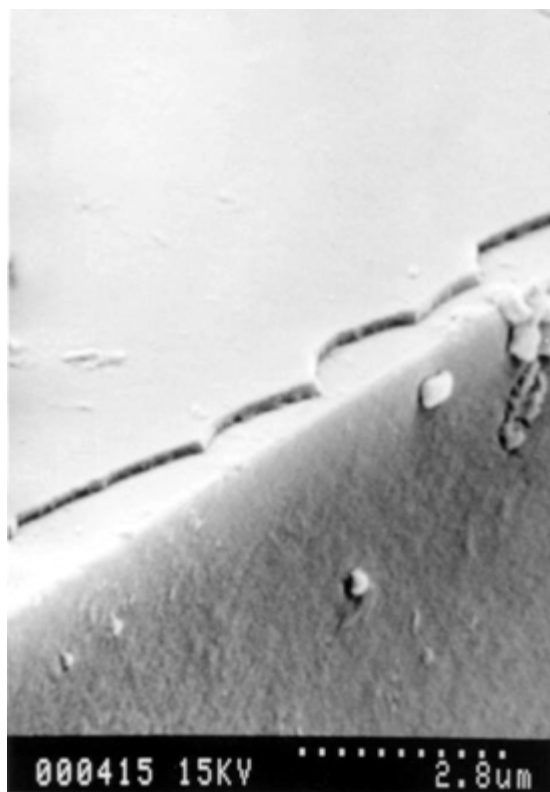


Fig. 5 B – SEM image of a perfectly transparent anatase film prepared at 673 K

the thin gel layers. The raw gels deposited on quartz wafers and PVA foils cut to fit to the Suprex cartridge were extracted by supercritical carbon dioxide. Layers (10 cycles) on quartz were, after this process, analysed for their organic carbon content. A value of $w = 8.3 \pm 0.7\%$ was obtained for a set of extracted samples. This value was found to be the limit of the extraction method. In our recent work⁵⁷ we demonstrated that small nano-particles formed in the process of supercritical fluid extraction tend to close (occlude) a significant number of surfactant molecules inside the forming micropores. Due to the quantities and geometrical constraints it is difficult, even for carbon dioxide to completely remove them from these very narrow channels.

The general XPS spectrum of electrons emitted from a gel after supercritical fluid extraction (range of binding energies 0–1000 eV) and the individual spectra of lines Ti 2p, O 1s, C 1s, revealed that oxygen and carbon were present (information depth of the method ~ 5 nm) in three chemically non-equivalent states ($C^a + C^b + C^c$). Values of binding energies of individual components of the spectra obtained by fitting and their possible interpretations are listed in Table 1. The highest surface abundance of the C^a was found as a characteristic feature of the SFE gel system. The non-polar hydrophobic head of the surfactant is pointing outward of the forming particles and thus groups such as CH_x , C–C, must predominate in the surface layer. An absolute identification was possible when comparing the binding energies and the Ti 2p line spectrum structure ($E_B = 458.6$ eV) with reference data for anatase. It seems that within (as also indicated for colloids⁵⁷) the structure of the gel after the SFE (but not thermally treated) the tetrahedral form of TiO_2 already exists. The formation of anatase from such gels at low temperatures, potentially enables a practical utilisation of cheap plastic substrates as supports for thin layers and their alternative *on-site* activation. An SEM of a typical thin layer (approximately 280 nm)

deposited on a PVA foil (not exposed to temperatures above 343 K) is shown in Figure 6-A. A layer deposited on a lower-quality PVA support (Figure 6-B) reflects perfectly the original surface corrugation as it could be seen in Figure 6-C. Such an “ancient brick wall” was amazingly still fairly transparent. In fact the large extent of fractures considerably increases the contribution of transport macropores and thus could be interesting for certain specific applications.

The thin layers (on quartz) treated by SFE and then calcined in the air at 673 K were found as excellent cut-off filters for the wavelength 365 nm by UV-VIS measurements. No blue-shift indication of the small particle quantum-dimension effects^{e.g.,19} was observed.

For the fabrication of a multifunctional photoactive supported membranes, plankton-based silica was chosen. The surface structure comprises an array of regular openings (about 1.3 μ m in diameter). This microstructured matrix is resistant to high temperature and pressure as well as most of mineral acids. Our aim was to close selectively the openings with the same solution used for the generation of the titania nanoparticulate layers by the surfactant templating. The membrane was successfully obtained with most of the properties identical to those of colloidal particles and thin layers. Figure 7 shows various stages of the silica rings blocking ranging from a complete absence to a nearly complete closure. The efficiency of this process invariably depends on kinetics of gelling and could be controlled through the viscosity of the reaction mixture. The conditions under which a complete “surface closure” is attained were found and such a membrane prepared. Its structure perfectly withstands SFE and after the thermal treatment at 773 K an extremely resistant and stable material is obtained. A surface microprobe confirmed that the original openings in the silica membrane are completely filled with Ti ions (from titania). The very promising application of this material could be foreseen for its utilisation as a photoactive catalytic membrane.

Table 1 – Measured values of binding energies E_B (eV) ± 0.2 eV and the standard matching

Line	E_B	Matching
Ti 2p	458.6	TiO_2
	530.1	TiO_2
O 1s	531.6	$-O-CH_2-$; C=O
	533.0	C–OH; (water)
C 1s	284.8	CH_x ; C–C (hydrocarbons)
	286.3	C–OH
	289.0	aromatic ring, $-CH_2-OH$; C–OOH

Conclusion

Thin titania layers were produced by the dip coating of various substrates (glass, quartz, PVA foils) with the intention to obtain highly transparent photoactive (anatase) films. The coating medium was obtained by the sol-gel transformation carried out in the core of reverse micelles of a non-ionic surfactant TX-100. The ratio of water-to-surfactant was kept low to limit the association of water molecules with terminal hydroxyl groups. In this way

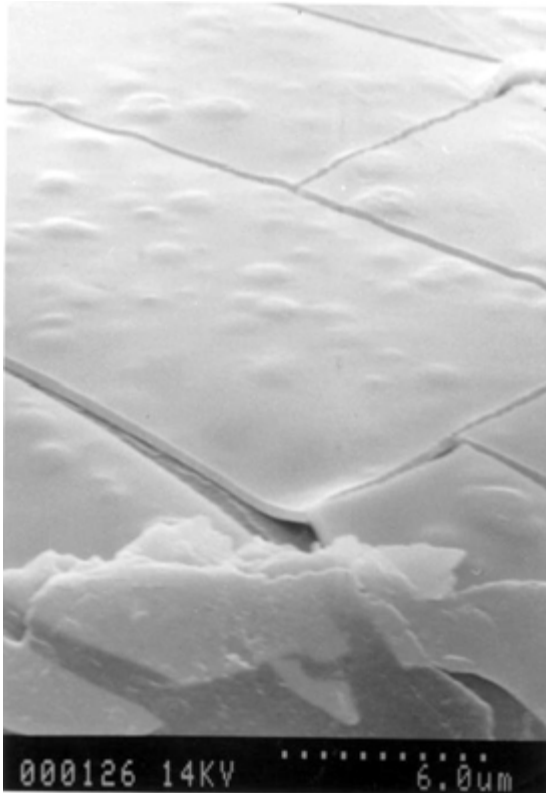


Fig. 6A – SEM image of a thin gel layer deposited on a surface of a PVA foil (mechanically damaged by severe bending)

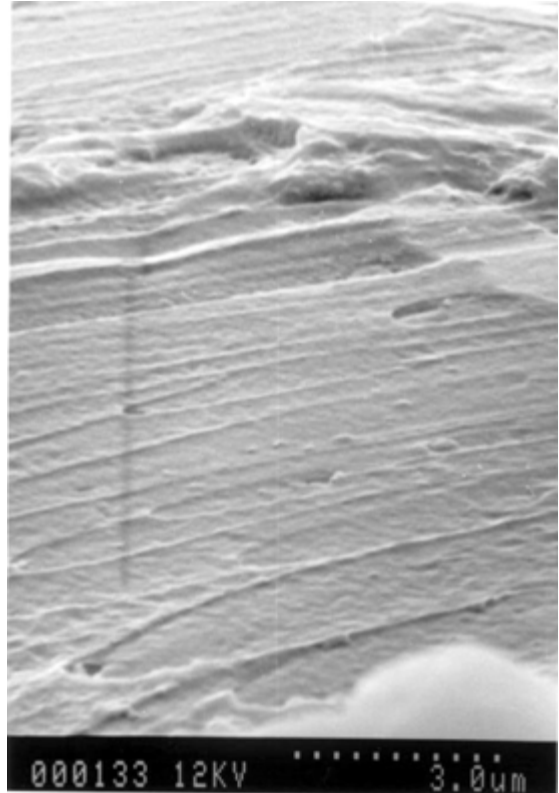


Fig. 6B – Corrugation of a surface of a lower quality PVA foil



Fig. 6C – SEM image of a thin gel layer deposited on such an irregular surface

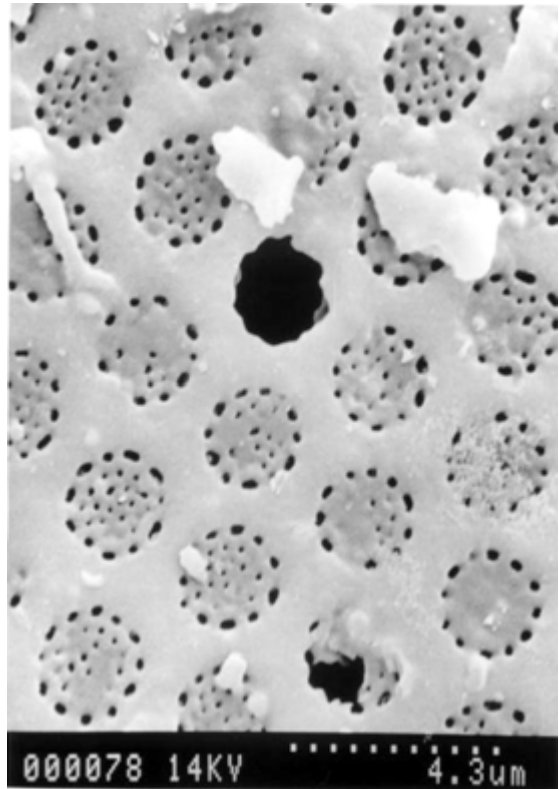


Fig. 7 – SEM image of the nanostructured titanie membrane supported on plankton based silica

transparent layers with little extent of surface defects were obtained. The exquisite transparency was a unique property of layers prepared by the surfactant templating. It is due to evolution of a polymeric –O–Ti–O–Ti–O– structure by polycondensation, which is competitive to hydrolysis of the initial alkoxide. Opaque layers formed of $\text{Ti}(\text{OH})_4$ precipitate were prepared for comparison also by the sol-gel method but in the surfactant-free environment.

The raw supported gels were thermally treated at eight isotherms up to 873 K. The anatase crystallographic structure became evident at 623 K as an increased background, at 723 K a sharp peak from the (101) plane diffraction was detected. The layers treated above 823 K were already less transparent due to larger extent of crystallisation. At 873 K the micro-crystals of anatase were already well developed and observable by electron microscopy. At this temperature (873 K) no phase transition of anatase to rutile had appeared.

Mechanism of the decomposition of the used surfactant was studied with the aim of determining the minimum temperature at which its content is substantially reduced while forming the TiO_2 matrix. Two significant stages were described, the first one associated with the oxygen attack on the lesser resistant hydrophilic chain; the second one starting at 673 K associated with the decomposition of the quinone fragment originating from the hydrophobic part of the molecule. At 823 K the organic carbon content in a layer was negligible.

SEM images and ellipsometry were used for estimation of the thickness of layers prepared by the multiple dip coating and then treated thermally in oxygen at 673 K. The film thickness varied roughly from 80 nm (2 cycles) to 400 nm (10 cycles) depending on the number of coating cycles. Porosity of a layer prepared in the three-cycle process was calculated to be 51 %. Some of the raw gel layers supported on quartz and PVA foils were extracted by supercritical carbon dioxide before any thermal treatment. It was shown that the SFE process significantly reduced the organic moiety, however, because of the geometrical constraints the complete extraction of the surfactant was not possible. XPS data confirmed that after the SFE the gels were already organised into the tetrahedral structure identical to that of anatase with the remaining surfactant molecules tending to be organised around the forming particles. Cheap and light plastic foils could be utilised as supports with possible *on-site* activation of the films. The thin layers with the anatase structure behaved as selective cut-off filters for wavelengths shorter than 365 nm.

We believe that the described titania layers could be utilised as highly active photo-oxidation catalysts or as a component basis for the new generation solar cells.^{59–63} The same applies for the nanostructured membranes having their potential utilisation in micro-membrane reactors with a separation and photoactive zones in one. The two introduced materials, that are the titania transparent thin nanoparticulate layers and the nanostructured supported membranes, are closely related through their physical and chemical properties. However, each of the material must be seen as an independent system in terms of its prospective applications.

ACKNOWLEDGEMENT

Authors wish to thank to Dr. A. Viana (University of Lisbon) for performing ellipsometry experiments and to Dr. Z. Bastl (J. Heyrovsky Institute of Physical Chemistry, CAS – Prague) for the XPS analysis.

References

1. Herrmann J. M., Tahiri H., Ait-Ichou Y., Lassaletta G., Gonzales-Felipe A. R., Fernandez A., *Appl. Catal. B* **13** (1997) 219.
2. Ohko Y., Fujishima A., Hashimoto K., *J. Phys. Chem.* **102** (1998) 1724.
3. Matthews R. W., *J. Phys. Chem.* **91** (1987) 3328.
4. Tada H., Tanaka M., *Langmuir* **13** (1987) 360.
5. Fernandez A., Lassaletta G., Jimenez V. M., Justo A., Gonzales-Felipe A. R., Herrmann J. M., Tahiri H., Ait-Ichou Y., *Applied Catalysis B* **7** (1995) 49.
6. Stafford U., Gray K. A., Kamat P. V., *J. Catal.* **167** (1997) 25.
7. Jenny B., Pichat P., *Langmuir* **7** (1991) 947.
8. Al-Ekabi H., Serpone N., *J. Phys. Chem.* **92** (1988) 5726.
9. Amalric L., Guillard C., Pichat P., *Res. Chem. Intermed.* **21** (1985) 33.
10. Krysova H., Krysa J., Macounova J., Jirkovsky J., *J. Chem. Technol. Biotechnol.* **72** (1998) 169.
11. Yamashita H., Nishiguchi H., Kamada N., Anpo M., Teraoka Y., Hatano H., Ehara S., Palmisano L., Scalfani A., Schiavello M., Fox M. A., *Res. Chem. Intermed.* **20** (1994) 815.
12. Muggli D. S., Lowery K. H., Falconer J. L., *J. Catal.* **180** (1998) 111.
13. Muggli D. S., Keyser S. A., Falconer J. L., *Catalysis Letters* **55** (1989) 129.
14. Shifu Ch., Xueli Ch., Yaowu T., Mengyue Z., *J. Chem. Technol. Biotechnol.* **73** (1998) 264.
15. Chum S. W., Jang J. Y., Park D. W., Woo H. Ch., Chung J. S., *Appl. Catal. B* **16** (1998) 235.
16. Herrman J. M., Disdier J., Pichat P., Malato S., Blanco J., *Appl. Catal. B* **17** (1998) 15.
17. Fujii H., Ohtaki M., Eguchi K., *J. Am. Chem. Soc.* **120** (1998) 6832.

18. *Pelizzeti E., Minero G., Borgarello E., Tinucci L., Serpone N.*, *Langmuir* **9** (1993) 2995.
19. *Anpo M., Shima T., Kodama S., Kubokawa Y.*, *J. Phys. Chem.* **91** (1987) 4305.
20. *Tsai S. J., Cheng S.*, *Catalysis Today* **33** (1997) 227.
21. *Ohtani B., Ogawa Y., Nishimoto S.*, *J. Phys. Chem.* **101** (1997) 3746.
22. *Lichtin N. N., Avudaithai M.*, *Res.Chem.Intermed.* **20** (1994) 755.
23. *Rivera A. P., Tanaka K., Hisanaga T.*, *Applied Catalysis B* **3** (1993) 37.
24. *Ferry J. L., Glaze W. H.*, *Langmuir* **14** (1998) 3551.
25. *Vinodgopal K., Hotchandani S., Kamat P. V.*, *J. Phys. Chem.* **97** (1993) 9040.
26. *Zhao G., Utsumi S., Kozuka H., Yoko T.*, *J. Mater. Sci.* **33** (1998) 3655.
27. *Anderson C., Bard A. J.*, *J. Phys. Chem.* **99** (1995) 9882.
28. *Verght M., Malkomes N., Staedler T., Mathee T., Richter U.*, *Thin Solid Films* **351** (1999) 42.
29. *Shin H., De Guire M. R., Heuer A. H.*, *J. Appl. Phys.* **83** (1998) 3311.
30. *Luciani L., Denoyel R.*, *Langmuir* **13** (1997) 7301.
31. *Ohya Y., Saiki H., Tanaka T., Takahasi Y.*, *J. Am. Ceram. Soc.* **79** (1996) 825.
32. *Keddie J. L., Braun P. V., Giannelis E. P.*, *J. Am. Ceram. Soc.* **77** (1994) 1592.
33. *Moriguchi I., Maeda H., Teraoka Y. And Kagawa S.*, *J. Am. Chem. Soc.* **117** (1995) 1139.
34. *Papoutsi D., Lianos P., Yanoulis Y., Koutsoukos P.*, *Langmuir* **10** (1994) 1684.
35. *Stathatos E., Lianos P., DelMonte F. Levy D., Tsiourvas D.*, *Langmuir* **13** (1997) 4295.
36. *Yoko T., Hu L., Kozuka H., Sakka S.*, *Thin Solid Films* **283** (1996) 188.
37. *Fajula F.*, Design and Engineering of Mesoporous Molecular Sieves – plenary lecture at the 5th Pannonian Symposium on Catalysis, Kazimier Dolny, Poland, May 31st to June 3rd, 2000, proceedings p. PL1.
38. *Peres-Durand S., Rouviere J., Guizard Ch.*, *Colloids and Surfaces A* **98** (1995) 251.
39. *Auvray L., Ayrat A., Ramsay J. D. F.*, *Faraday Discussions* **101** (1995) 235.
40. *Lopez T., Sanchez E., Bosch P., Meas Y., Gomez R.*, *Mater. Chem. and Physics* **32** (1992) 141.
41. *Kresge C. T., Leonowicz M. E., Roth W. J., Vartuli J. C., Beck J. C.*, *Nature* **359** (1992) 710.
42. *Doherty S., Fitzmaurice D.*, *J. Phys. Chem.***100** (1996) 10732.
43. *Boschloo G., Fitzmaurice D.*, *J. Phys. Chem.B*, **103** (1999) 7860.
44. *Kawi S., Wai Lai M.*, *Chem. Commun.*, **13** (1998) 1407.
45. *Kawi S., Wai Lai M.*, *Chemtech* **28** (1998) 26.
46. *Anderson B., Olofsson G.*, *J. Chem. Soc., Faraday Trans 1.* **84** (1988) 4087.
47. *Jha R., Ahluwalia J. C.*, *J. Phys. Chem.* **95** (1991) 7782.
48. *Funasaki N., Hada S., Neya S.*, *Bull. Chem. Soc. Jpn.* **62** (1989) 1725.
49. *Brown W., Rymden R., van Stam J., Almgren M., Svensk G.*, *J. Phys. Chem.* **93** (1989) 2512.
50. *Zhu D. M., Feng K. I., Schelly Z. A.*, *J. Phys. Chem.* **96** (1992) 2382.
51. *Imai H., Hirashima H., Awazu K.*, *Thin Solid Films* **351** (1999) 91.
52. *Maier W. F., Tilgner I. C., Wiedorn M., Che H. K., Zichfreund A., Sell R.*, *Adv. Matter.* **5** (1993) 730.
53. *Mitsuda K., Kimura H., Murahasi T.*, *J. Mater. Sci.* **24** (1989) 413.
54. *Suresh C., Biju V, Mukundan P., Warriar K.G.K.*, *Polyhedron* **17** (1998) 3131.
55. *So W. W., Park S. B., Moon S. J.*, *J. Mater. Sci. Letters* **17** (1998) 1219.
56. Powder Diffraction File of the JCPDS – International Centre for Diffraction Data, Swathmore – Pennsylvania, 1998.
57. *Kluson P., Kacer P., Cajthaml T., Kalaji M.*, *J. Mater. Chem.* **11** (2001) 644.
58. *Kormann C., Bahnemann D. W., Hoffmann M. W.*, *J. Phys. Chem.* **92** (1988) 5196.
59. *Shklover V., Nazeeruddin M. K., Zakeeruddin S. M., Barbe C., Kay A., Haibach T., Steurer W., Hermann R., Nissen H.U., Grätzel M.*, *Chem. Mater.* **9** (1997) 430.
60. *Bach U., Lupo D., Comte P., Moser J. E., Weissörtel F., Salbeck J., Spreitzer H., Grätzel M.*, *Nature* **395** (1998) 583.
61. *Barbe Ch., Arendse F., Comte P., Jirousek M., Lenzmann F., Shklover V., Grätzel M.*, *J. Am. Ceram. Soc.* **80** (1997) 3157.
62. *Burnside S. D., Shklover V., Barbe Ch., Comte P., Arendse F., Brooks K., Grätzel M.*, *Chem. Mater.* **10** (1998) 2419.
63. *Hagfeldt A., Björksten U., Grätzel M.*, *J. Phys. Chem.* **100** (1996) 8045.